Journal of Molecular Liquids 319 (2020) 114327

Contents lists available at ScienceDirect

Journal of Molecular Liquids

journal homepage: www.elsevier.com/locate/molliq

Unusual origin of choline phenylalaninate ionic liquid nanostructure

Shurui Miao [a], Jared Wood [a], Haihui Joy Jiang [a], Silvia Imberti [b], Rob Atkin [c], Gregory Warr [a,*]

[a] School of Chemistry and Sydney Nano Institute, The University of Sydney, NSW 2006, Australia
[b] STFC, Rutherford Appleton Laboratory, Didcot, UK
[c] School of Molecular Sciences, The University of Western Australia, WA 6009, Australia

ARTICLE INFO

Article history:
Received 20 July 2020
Received in revised form 11 September 2020
Accepted 13 September 2020
Available online 17 September 2020

Keywords:
Ionic liquids
Biocompatible
Neutron diffraction
Amphiphilic nanostructure
Self-assembly

ABSTRACT

Choline amino acid ionic liquids have received much attention recently due to their environmental friendliness and low toxicity. Some of these ionic liquids have shown outstanding capacity for biomass and coal pretreatment, yet it remains unclear what structural features underpin performance. Despite sharing many structural features with other choline amino acid ionic liquids proven to be effective at lignin extraction, choline phenylalaninate (ChPhe) is surprisingly among the poorest solvents at such application. Using multi-contrast neutron diffraction we show that the liquid nanostructure of ChPhe – consisting of apolar domains in a continuous polar network – primarily consists of small clusters stabilised by inter-anion hydrogen bonds between amine and carboxylate groups. Within the apolar regions, phenyl side-chain rings adopt no preferred arrangements, signaling the absence of π-π stacking, but instead show evidence of competing cation-π interactions. This is the first example of self-assembled ionic liquid nanostructure not of solvophobic origin. The unusual suite of interactions also explains its water miscibility but inability to retain nanostructure upon water dilution, as well as its poor performance for biomass pretreatment, and provides a new strategy by which to engineer and tune ionic liquid nanostructure for the design of application-specific, renewable solvent systems.

1. Introduction

Room temperature ionic liquids (ILs) are liquids composed entirely of ions, which have gained increasing attention across many fields including catalysis [1], electrochemistry [2], energy storage [3], extraction [4], biochemistry [5], and lubrication [6]. The physical and solvent properties required for this range of applications is diverse, but ILs' tunability through both cation and anion structures enables them to be more effectively designed for purpose. Broadly, ionic liquids are classified as protic or aprotic, depending on the synthesis method [7]. A key feature of ILs is that they exhibit nanoscale structure when the cation alkyl chain contains 4 or more carbons in aprotic ILs, or 2 or more carbons in protic ILs. This nanostructure arises from strong electrostatic interactions between cation and anion charge groups leading to the formation of a polar domain from which the cation alkyl chains are solvophobically excluded, clustering into separate apolar regions [8]. These polar and apolar domains frequently percolate through the liquid in a bicontinuous, sponge-like structure [9]. There are nanostructure variations, including tricontinuous ILs [10], and those in which the alkyl chain is part of the anion [11], but the origin of the nanostructure is always solvophobic. Nanostructured ILs can often dissolve a wider variety of solutes than either homogenous ILs or molecular liquids, and are excellent at facilitating amphiphilic self-assembly [12].

The widespread use of ILs is limited by concerns about cost and biocompatibility. Compared to aprotic ILs, protic ILs are much cheaper and less toxic, as halogenated species can be avoided [7]. However, the majority of these remain non-biodegradable [13]. The recent discovery of choline-based amino acid ILs have improved solvent greenness [14], retaining the advantages of protic ILs while improving biocompatibility and being non-toxic to most living organisms [15,16].

Previous work has shown choline ILs with a variety of bio-based and synthetic carboxylate and amino acid anions exhibit differing degrees of long-range amphiphilic nanostructure [11,17–19]. This is signalled by the presence of a low angle "pre-peak" in small-angle scattering patterns, which reflects quasi-periodic ordering of polar and non-polar domains beyond the shorter range charge ordering, and is widely documented in conventional protic and aprotic ILs [8,20,21]. Among protic ILs, amphiphilic nanostructure is strongly linked to solvency for organic solutes including alkanols [22] and various aromatic species including model lignin residues [23], and this is generally also the case for choline ILs [11].

Choline phenylalaninate (ChPhe) differs from most ILs in that its apolar moiety is aromatic. This raises the prospect of π-π stacking that may enhance apolar aggregation and ordering of the nanostructure, and for which some support is afforded by simulations [24]. Unlike other nanostructured ILs however, the pre-peak disappears upon

* Corresponding author.
E-mail address: gregory.warr@sydney.edu.au (G. Warr).

https://doi.org/10.1016/j.molliq.2020.114327
0167-7322/

dilution with water, indicating disruption of the amphiphilic nanostructure [11], yet ChPhe remains miscible with alkanols up to 1-octanol with these mixtures exhibiting enhanced, long-range amphiphilic order. This suggests an adaptive solvent nanostructure that can accommodate a diverse range of solutes. It is thus surprising that ChPhe was the least effective extraction solvent for lignin from rice straw among 8 choline amino acid ILs [25]. Despite having a more pronounced nanostructure peak, ChPhe is 33% less effective at lignin removal than choline lysinate. To understand how to design and optimise choline IL systems, we must unravel structure-property relationships and the role of liquid nanostructure in determining solvent behaviour.

In this study we investigate the origin of the liquid nanostructure of ChPhe utilising neutron liquid diffraction, fitted using Empirical Potential Structure Refinement (EPSR). We identify the key intermolecular interactions that stabilise its unique nanostructure. Details on a molecular level are reflected in the macroscopic behaviour exemplified by miscibility, providing insights to optimise and control the solvent properties for future design of green, task-specific solvent systems.

2. Materials and methods

Preparation of hydrogenous ChPhe (H-ChPhe) was based on published method [26]. DL-phenylalanine (99%, Fluka) and choline hydroxide aqueous solution (~46 wt%, Aldrich), were used as received. The concentration of choline hydroxide solution was determined through titration before use. It was diluted to 20 wt% before added dropwise to a cooled 20 wt% mixture of DL-phenylalanine powder in water, under vigorous stirring. The reaction was kept on an ice bath (<10 °C) and stirred overnight under ambient conditions. Upon completion, phenylalanine should be in ~5 mol% excess and a clear aqueous solution is obtained. Bulk water was removed on a rotary evaporator (40 °C, 10 mbar), excess phenylalanine was precipitated and removed by filtration in acetonitrile:methanol = 9:1 v/v solution. The liquid phase was collected with solvents removed using a rotary evaporator; drying of the residual water was performed under high vacuum at room temperature for >48 h. Water content of final ChPhe was confirmed to be <1 wt% using Karl-Fischer titration (Metrohm 784 KFP Titrino). Dried ChPhe has a light amber appearance due to trace impurity from the choline hydroxide reagent (undetectable by ^{1}H NMR - see Fig. S2). Throughout the preparation, NMR is employed to monitor various hydrogen environments to ensure desired 1:1 ion ratio was achieved within 1 mol%.

d_9-ChPhe for neutron experiments was prepared using d_9-choline chloride (d_9-ChCl, 98%, Cambridge Isotope), which was ion-exchanged on a resin (Amberlite IRA-400 for hydroxide, 25 mL) to d_9-choline hydroxide (d_9-ChOH). Before use, resins were washed with concentrated NaOH aqueous solutions five times. Silver test (0.2 M $AgNO_3$ and 0.25 M HNO_3 in water) confirmed negligible amount of chloride remained in the resins, subsequent water (Milli-Q) rinse was performed until pH returned to neutral. 5 g of d_9-ChCl was dissolved in 50 mL of H_2O/methanol 1:1 v/v mixture and loaded to 200 mL of resins using the same solvent mixture as eluent. Eluents were collected in fractions and all fractions with basic pH were combined (pH > 7.5). A small volume of the obtained solution was titrated, and a separate sample was analysed using ICP-MS using high purity NaCl as standards (between 0.5 and 5000 ppm). 98% exchange yield was achieved with <10 ppm chloride. d_9-ChPhe was prepared identically to H-ChPhe with the same DL-phenylalanine.

d_{12}- and d_3-ChPhe were obtained through H/D exchange of exchangeable protons within d_9-ChPhe and H-ChPhe samples. Deuterium oxide D_2O (99%, Cambridge Isotope) was added to ChPhe in 3:1 volume ratio. Resulting mixture was stirred for 5 min before drying on rotary evaporator (40 °C, 10 mbar). Mass was monitored to ensure bulk D_2O were removed. This process was repeated 5 times, the final sample was dried under high vacuum at room temperature for >48 h. All samples were sealed and stored under nitrogen.

Neutron diffraction was collected on SANDALS beamline at ISIS Neutron and Muon Source (Rutherford Appleton Laboratories, UK). The neutron wavelength ranges between 0.05 and 4.95 Å, allowing access to the q-range of between 0.05 and 50 $Å^{-1}$. Samples were contained in null scattering $Ti_{0.68}Zr_{0.32}$ flat plate cells with total capacity of 1 mL. All samples were measured under vacuum at 296 K for 6 h each. Mass were monitored to ensure no loss of sample under vacuum. Data reduction was performed using GUDRUN according to local procedures. The Empirical potential structure refinement (EPSR) package was used to fit the normalized data. The simulation box was composed of 500 choline cations and 250 of each of D- and L-phenylalaninate anions, 60 Å along each axis. Atom labelling and initial Lennard-Jones parameters are provided in ESI (Fig. S1 and Table S1). The simulation box was driven to fit all 4 diffraction patterns (different isotopic substitutions) simultaneously as shown in Fig. 1a), and the size of the simulation box was ensured to be more than twice the size of the largest experimental structural feature. Atomic density of each system was calculated based on experimental density of hydrogenous ChPhe measured by DMA 35 N densitometer (Anton Paar) at 23 °C. All analyses were performed over 2777 frames of data accumulation on fully-converged simulation.

3. Results

Fig. 1a) shows the experimental neutron diffraction patterns from four distinct H/D isotopic substitutions (i.e. neutron contrasts) of ChPhe, together with the best fit obtained to a single liquid model simulated using EPSR. The key experimental structural feature is the prominent peak observed at 0.35 $Å^{-1}$ in the two partially deuterated samples, which corresponds closely to the pre-peak position previously reported by small angle X-ray scattering [17]. This peak corresponds to a periodicity of 18 Å, which is much greater than individual ion dimensions (<8 Å), but less than one third of the side-length of the simulation box. The fitted diffraction patterns are in good agreement with experiment, except for the intensity of this low-q peak for the fully hydrogenous contrast. This may be a consequence of being near the resolution limit of the technique (~0.2 $Å^{-1}$), leading to some error in inelastic scattering correction, or due to the presence of a small amount of water absorbed from air during sample storage and handling. However, as EPSR provides atomic resolution and the structural refinement is performed on the molecular scale, our interpretation based on inter-ion interactions should not be affected. Fig. 1b) shows the molecular structure of ChPhe, with labels of important atomic sites used throughout the rest of the discussion.

H-bonds re-enforce electrostatic interactions in protic ionic liquids and thus contribute to the solvophobic segregation of apolar groups. Unlike electrostatic interactions, H-bonds are directional, and thus affect the polar network structure in many ILs [9,27–29]. We have surveyed the radial distribution functions (RDFs) of all H-bond donor/acceptor combinations in ChPhe (Figs. 2 and S3), and identified only two with significant nearest-neighbour peaks in the characteristic H-bonding distance range, r = 1.5–1.8 Å [30]. These are shown in Fig. 2 (all others shown in Fig. S3).

The dominant H-bond interaction is that between the cation hydroxyl hydrogen (H_O) and carboxylate oxygens (O_1) of the anion with a coordination number of 0.81, which is consistent with experimental results obtained from IR spectroscopy and theoretical studies [24,31–34]. This implies about 80% of choline cations are ion-paired to phenylalaninate via a short, linear H-bond. However, a surprising H-bond is also observed between the amine hydrogens (H_2) and carboxylate O_1 on the anions, such that almost one quarter of the amino hydrogens are also H-bonded (i.e. coordination number is 0.23). This is due to a deficit of H-bond donors on the cation; there are fewer choline hydroxyls than carboxylate oxygens in ChPhe due to the stoichiometry, so amine moieties can also interact with carboxylates, overcoming the electrostatic repulsion. This inter-anion (H_2-O_1) H-bond is longer on average, with a broader distribution of bond lengths and angles due to

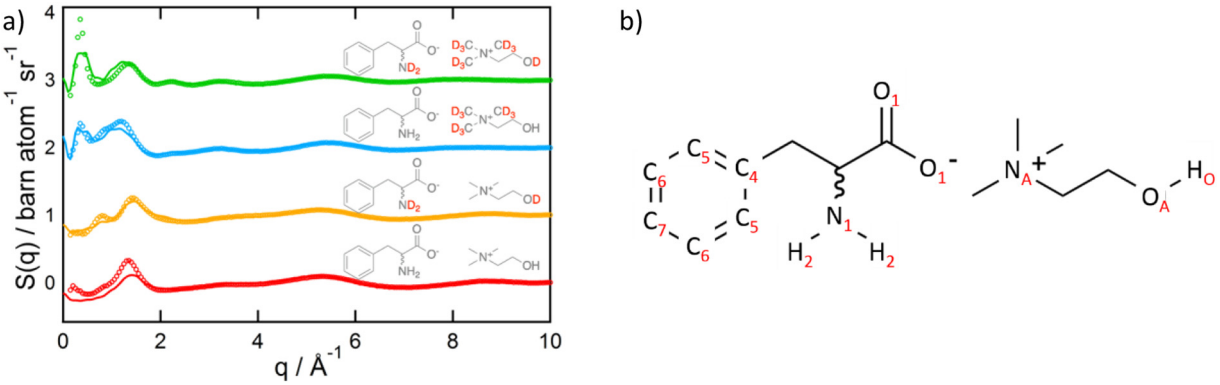

Fig. 1. a) Experimental (hollow circles) and fitted (solid line) neutron diffraction patterns of ChPhe IL with 4 different H/D contrasts between 0 and 10 Å^{-1}. The corresponding isotopic labelling (deuteration) are shown above each curve. Curves are offset for clarity. b) Molecular structure of ChPhe, showing labels of important atomic sites discussed in the text.

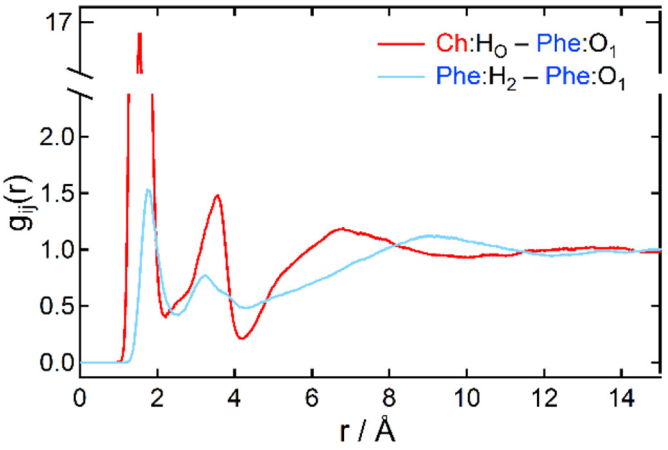

Fig. 2. Radial distribution functions of significant hydrogen bond forming atom-pairs in ChPhe.

the influence of electrostatic repulsions [33–35]. In this respect, amino acid anions mirror the recently-reported behaviour of pyridinium and piperidinium aprotic ILs with hydroxyl-terminated cation alkyl chains, in which cation-cation and cation-anion H-bonding can be tuned by changing both cation charge delocalisation and anion donor quality [29].

In addition to the short-range directional H-bonds, mid- to long-range electrostatic interaction are key to many unique physicochemical properties of ILs. Fig. 3a) shows the radial distribution functions of all atomic sites carrying partial negative charges around the choline quaternary ammonium nitrogen. This shows that the negative carboxylate oxygens (O_1) are most strongly and closely associated with the cation quaternary ammonium (N_A). Additionally, both the anion amine nitrogen (N_1) and cation hydroxyl oxygen (O_A) also associate strongly with the quaternary ammonium, but at larger average separations. (The secondary peak at 6.5 Å is for N_A-N_1 is simply a consequence of the N_A-O_1 interaction and the amino acid anion geometry.)

Fig. 3b) depicts the spatial distribution function (SDF) of carboxylate around N_A, showing the 30% probability surface where an O_1 atom is most likely to be found. This demonstrates that O_1 can access the gaps between methyl moieties and embed itself into the delocalised positive charge [36].

Among reported choline amino acid ILs, ChPhe is unique due to the aromatic side-chain of its anion. This has the potential for attractive π-π stacking, which may enhance solvophobic segregation and yield more ordered amphiphilic nanostructure. Previous small angle x-ray scattering studies have shown both ChPhe and choline homophenylalanine are nanostructured with aromatic-rich domains [11,17]; This, combined with their unexpectedly high liquid densities, led to π-π stacking being proposed to justify the observed molecular segregation [17]. This is also consistent with *ab initio* simulation of ChPhe clusters (containing up to 15 ion pairs), where parallel stacking of phenyl moieties was identified [24]. A similar experimental study of IL/benzene mixtures using neutron diffraction and EPSR has revealed a weak preference for perpendicular stacking among aromatics [37].

Careful examination of RDFs between all combinations of distinct phenyl carbons (Fig. 4a)) yielded no correlations that are comparable to even the weaker of the two H-bonds in this system. Instead, a small, very broad peak is observed between 4 and 8 Å, suggesting

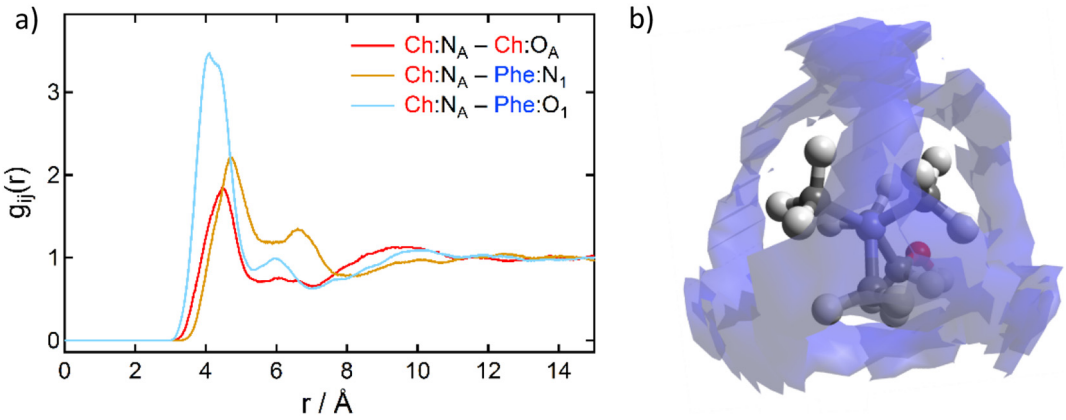

Fig. 3. a) Radial distribution functions of key electrostatic interactions around choline; b) corresponding spatial distribution function (30% probability surface) of anion carboxylate oxygen (O_1) around cation quaternary nitrogen (N_A), hydrogen atoms of methyl groups are omitted for clarity.

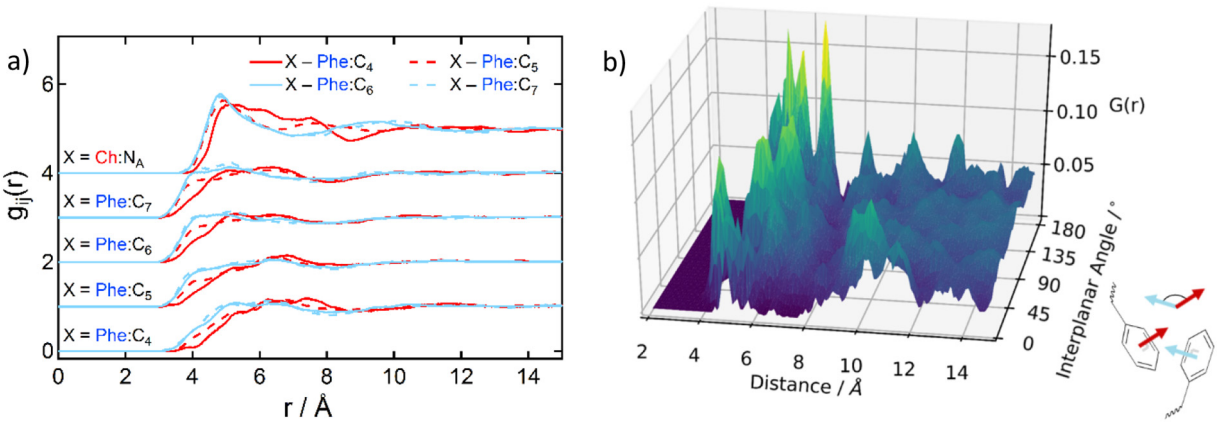

Fig. 4. a) RDFs between distinct carbons of the anion phenyl ring, and with the quaternary ammonium of choline (Ch:N_A). Curves are offset for clarity. b) Angular radial distribution function plot between phenyl moieties, distance is defined between centre of masses, angle is defined between the normal axis of the rings and g (r) is the correlation intensity. Both a) and b) were accumulated over 2777 simulation frames.

weak, non-specific association of the aromatic groups. The similarities between all four sets of RDFs between phenyl carbons reflect the absence of preferred parallel, anti-parallel or perpendicular arrangements of the rings. This is also evident in the RDFs between phenyl ring centres-of-mass, shown as a function of angle between rings in Fig. 4b). The broad nearest-neighbour peak (at 4–8 Å) is consistent with ring association and some apolar clustering, with the distance of closest approach between centres-of-mass, and hence packing, depending on relative orientation. However, no distinct peak indicating stacking in either parallel (0°, 180°) or perpendicular (90°) orientations is observed [24,37].

In contrast with the negligible correlations between phenyl ring carbons, Fig. 4a) reveals a pronounced correlation peak between phenyl rings and the choline ammonium nitrogen. This cation-π correlation is also clear in an SDF representation (Fig. 5), which depicts the preferred (30% probability surface) location of choline quaternary nitrogens on either side of a phenyl moiety, perpendicular to the ring plane, where the electron-rich π system is located. Although the cation-π interaction is weak compared to H-bonds, it is sufficient to overcome any preference for π-π stacking and disrupts, rather than enhances, the formation of extended apolar domains. This may also explain the discrepancy between our results and earlier theoretical calculations [24].

A cation-π interaction has been predicted for imidazolium cations and aromatic amino acid anions [38], whereby the cation H-bonds to the carboxylate group, simultaneously establishing cation-π contact with the aromatic side-chain. This analysis shows that the choline cation can also interact with phenylalaninate by establishing a similar geometry; the cation hydroxyl and anion carboxylate are most strongly associated by H-bonding, leaving the cation ammonium available to engage with phenyl side-chains. This is further supported by NMR study of eight aromatic side-chain ILs, including ChPhe [39].

Despite the absence of π-π stacking, and a diminished solvophobic effect due to cation-π interactions, molecular segregation must exist beyond nearest neighbours to account for low-q features observed in neutron diffraction (Fig. 1) and small-angle X-ray scattering [11,17]. By using nearest-neighbour interaction distances extracted from corresponding RDFs, we can characterise the extent of clusters and networks formed within the liquid to gain insights into the origins of long-range ordering in ChPhe.

Fig. 6 shows the probability of finding an ion within various types of clusters of different sizes. Details of cluster definition and nearest-neighbour cut-off are provided in Table S3. Using nearest-neighbour correlations between quaternary nitrogen and carboxylate oxygen charge centres leads to a single, continuous polar network spanning the entire simulation box (1000 ions), similar to those seen in other ILs [20,21]. This contrast with finite clusters formed by counting only H-bonded nearest neighbours, which contain at most ~20 ions and with only small clusters of 2–10 ions more likely than random clustering. Clusters consisting of only cation-anion H-bonds are smaller still,

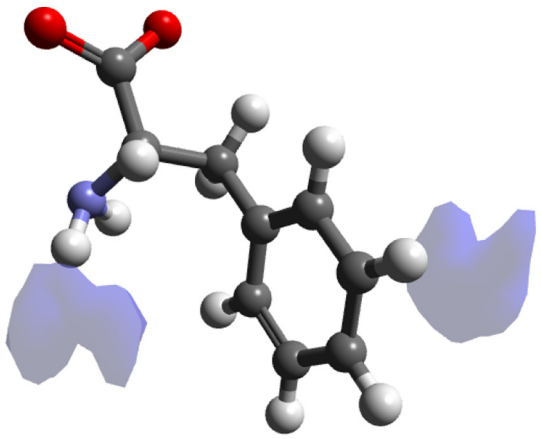

Fig. 5. The SDF (30% probability surface) of quaternized ammonium nitrogen (cation) around phenyl moieties showing a clear preferred location perpendicular to the aromatic ring, which optimises ion-quadrupole interaction.

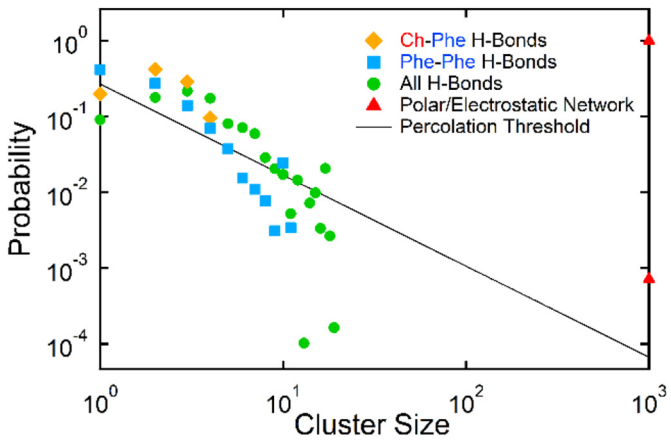

Fig. 6. Cluster analysis of various interactions, probability is the fraction of ions in a cluster of size n defined by separation distances. Black line is the theoretical percolation threshold ($p = n^{-1.2}/3.74$).

and only contain up to 4 ions in total, underscoring the importance of anion-anion H-bonding in the liquid nanostructure. This means that, although the solvophobic effect is offset by countervailing cation-π interactions, molecular segregation is present in ChPhe, and anion-rich domains are sustained by inter-anion hydrogen bonds.

4. Conclusions

Multi-contrast neutron diffraction patterns fitted by a large (500 ion pair) simulation using empirical potential structure refinement has shown that the amphiphilic nanostructure in this IL is not a consequence of solvophobic exclusion of aromatic groups as occurs with non-polar, alkyl moieties. Instead, multiple phenylalaninate anions form large clusters by inter-anion H-bonds between their amine and carboxylate functional groups. This is enabled by the continuous network formed by the cation and anion charge centres, which shields electrostatic repulsions between H-bonding anions. Any solvophobic contribution to phenyl ring associations is diminished by cation-π interactions.

Contrary to earlier suggestions of π-π stacking being a significant cause of molecular segregation [17,24], our analysis has demonstrated the unique structural contribution of the phenyl side-chains arises through cation-π interactions. As a consequence of this attraction between charged and apolar moieties, the solvophobic effect is greatly suppressed in ChPhe, giving rise to a less ordered amphiphilic nanostructure relative to conventional ILs [9,21]. This explains why the long-range nanostructure of ChPhe is easily disrupted by water while remaining miscible [11]. The reported poor extraction efficiency and high residue recovery percentage of ChPhe during biomass pretreatment [25], can also be attributed to this lack of strictly solvophobic domains.

CRediT authorship contribution statement

Shurui Miao: Investigation, Formal analysis, Writing - original draft, Visualization. **Jared Wood:** Software, Validation. **Haihui Joy Jiang:** Formal analysis, Resources. **Silvia Imberti:** Investigation, Formal analysis, Resources. **Rob Atkin:** Conceptualization, Funding acquisition, Writing - review & editing. **Gregory Warr:** Conceptualization, Resources, Supervision, Project administration, Funding acquisition, Writing - review & editing.

Declaration of competing interest

The authors declare that they have no known competing financial interests or personal relationships that could have appeared to influence the work reported in this paper.

Acknowledgement

This work was supported by an Australian Research Council (ARC) Discovery Grant. The neutron diffraction was performed at ISIS Neutron and Muon Source (RAL, UK), SANDALS beamline, under proposal RB1810865. SM thanks Australian Government for an RTP scholarship and AINSE for a PGRA.

Appendix A. Supplementary data

Supplementary data to this article can be found online at https://doi.org/10.1016/j.molliq.2020.114327.

References

[1] V.I. Parvulescu, C. Hardacre, Catalysis in ionic liquids, Chem. Rev. 107 (6) (2007) 2615–2665.
[2] H.T. Liu, Y. Liu, J.H. Li, Ionic liquids in surface electrochemistry, Phys. Chem. Chem. Phys. 12 (8) (2010) 1685–1697.
[3] M. Watanabe, M.L. Thomas, S.G. Zhang, K. Ueno, T. Yasuda, K. Dokko, Application of ionic liquids to energy storage and conversion materials and devices, Chem. Rev. 117 (10) (2017) 7190–7239.
[4] T.Q. To, K. Shah, P. Tremain, B.A. Simmons, B. Moghtaderi, R. Atkin, Treatment of lignite and thermal coal with low cost amino acid based ionic liquid-water mixtures, Fuel 202 (2017) 296–306.
[5] P. Attri, P. Venkatesu, A. Kumar, Water and a protic ionic liquid acted as refolding additives for chemically denatured enzymes, Org. Biomol. Chem. 10 (37) (2012) 7475–7478.
[6] L. Mu, Y. Shi, X. Guo, T. Ji, L. Chen, R. Yuan, L. Brisbin, H. Wang, J. Zhu, Non-corrosive green lubricants: strengthened lignin-[choline][amino acid] ionic liquids interaction via reciprocal hydrogen bonding, RSC Adv. 5 (81) (2015) 66067–66072.
[7] T.L. Greaves, C.J. Drummond, Protic ionic liquids: properties and applications, Chem. Rev. 108 (1) (2008) 206–237.
[8] R. Hayes, G.G. Warr, R. Atkin, Structure and nanostructure in ionic liquids, Chem. Rev. 115 (13) (2015) 6357–6426.
[9] R. Hayes, S. Imberti, G.G. Warr, R. Atkin, Pronounced sponge-like nanostructure in propylammonium nitrate, Phys. Chem. Chem. Phys. 13 (30) (2011) 13544–13551.
[10] T.L. Greaves, D.F. Kennedy, Y. Shen, A. Hawley, G.H. Song, C.J. Drummond, Fluorous protic ionic liquids exhibit discrete segregated nano-scale solvent domains and form new populations of nano-scale objects upon primary alcohol addition, Phys. Chem. Chem. Phys. 15 (20) (2013) 7592–7598.
[11] S. Miao, R. Atkin, G.G. Warr, Amphiphilic nanostructure in choline carboxylate and amino acid ionic liquids and solutions, Phys. Chem. Chem. Phys. 22 (6) (2020) 3490–3498.
[12] T.L. Greaves, A. Weerawardena, I. Krodkiewska, C.J. Drummond, Protic ionic liquids: physicochemical properties and behavior as amphiphile self-assembly solvents, J. Phys. Chem. B 112 (3) (2008) 896–905.
[13] A. Jordan, N. Gathergood, Biodegradation of ionic liquids - a critical review, Chem. Soc. Rev. 44 (22) (2015) 8200–8237.
[14] Q.-P. Liu, X.-D. Hou, N. Li, M.-H. Zong, Ionic liquids from renewable biomaterials: synthesis, characterization and application in the pretreatment of biomass, Green Chem. 14 (2) (2012) 304–307.
[15] X.-D. Hou, Q.-P. Liu, T.J. Smith, N. Li, M.-H. Zong, Evaluation of toxicity and biodegradability of cholinium amino acids ionic liquids, PLoS One 8 (3) (2013) e59145–e59148.
[16] M. Petkovic, J.L. Ferguson, H.Q.N. Gunaratne, R. Ferreira, M.C. Leitao, K.R. Seddon, L.P.N. Rebelo, C.S. Pereira, Novel biocompatible cholinium-based ionic liquids-toxicity and biodegradability, Green Chem. 12 (4) (2010) 643–649.
[17] M. Campetella, D.C. Martino, E. Scarpellini, L. Gontrani, Low-Q peak in X-ray patterns of choline-phenylalanine and -homophenylalanine: a combined effect of chain and stacking, Chem. Phys. Lett. 660 (2016) 99–101.
[18] M. Campetella, S. De Santis, R. Caminiti, P. Ballirano, C. Sadun, L. Tanzi, L. Gontrani, Is a medium-range order pre-peak possible for ionic liquids without an aliphatic chain? RSC Adv. 5 (63) (2015) 50938–50941.
[19] L. Tanzi, F. Ramondo, R. Caminiti, M. Campetella, A. Di Luca, L. Gontrani, Structural studies on choline-carboxylate bio-ionic liquids by x-ray scattering and molecular dynamics, J. Chem. Phys. 143 (11) (2015).
[20] H.K. Kashyap, J.J. Hettige, H.V.R. Annapureddy, C.J. Margulis, SAXS anti-peaks reveal the length-scales of dual positive–negative and polar–apolar ordering in room-temperature ionic liquids, Chem. Commun. 48 (5103) (2012) 5103–5105.
[21] R. Hayes, S. Imberti, G.G. Warr, R. Atkin, Amphiphilicity determines nanostructure in protic ionic liquids, Phys. Chem. Chem. Phys. 13 (8) (2011) 3237–3247.
[22] H.J. Jiang, P.A. FitzGerald, A. Dolan, R. Atkin, G.G. Warr, Amphiphilic self-assembly of alkanols in protic ionic liquids, J. Phys. Chem. B 118 (33) (2014) 9983–9990.
[23] H.J. Jiang, S. Imberti, B.A. Simmons, R. Atkin, G.G. Warr, Structural design of ionic liquids for optimizing aromatic dissolution, ChemSusChem 12 (1) (2019) 270–274.
[24] M. Campetella, E. Bodo, M. Montagna, S. De Santis, L. Gontrani, Theoretical study of ionic liquids based on the cholinium cation. Ab initio simulations of their condensed phases, J. Chem. Phys. 144 (10) (2016) 104504–104508.
[25] X.D. Hou, T.J. Smith, N. Li, M.H. Zong, Novel renewable ionic liquids as highly effective solvents for pretreatment of rice straw biomass by selective removal of lignin, Biotechnol. Bioeng. 109 (10) (2012) 2484–2493.
[26] S. De Santis, G. Masci, F. Casciotta, R. Caminiti, E. Scarpellini, M. Campetella, L. Gontrani, Cholinium-amino acid based ionic liquids: a new method of synthesis and physico-chemical characterization, Phys. Chem. Chem. Phys. 17 (2015) 20687–20698.
[27] K. Fumino, A. Wulf, R. Ludwig, Hydrogen bonding in protic ionic liquids: reminiscent of water, Angew. Chem. Int. Ed. 48 (2009) 3184.
[28] R.P. Matthews, T. Welton, P.A. Hunt, Competitive pi interactions and hydrogen bonding within imidazolium ionic liquids, Phys. Chem. Chem. Phys. 16 (7) (2014) 3238–3253.
[29] T. Niemann, J. Neumann, P. Stange, S. Gartner, T.G.A. Young, D. Paschek, G.G. Warr, R. Atkin, R. Ludwig, The double-faced nature of hydrogen bonding in hydroxy-functionalized ionic liquids shown by neutron diffraction and molecular dynamics simulations, Angew. Chem. Int. Ed. 58 (37) (2019) 12887–12892.
[30] R. Hayes, S. Imberti, G.G. Warr, R. Atkin, The nature of hydrogen bonding in protic ionic liquids, Angew. Chem. Int. Ed. 52 (17) (2013) 4623–4627.
[31] M. Campetella, E. Bodo, R. Caminiti, A. Martino, F. D'Apuzzo, S. Lupi, L. Gontrani, Interaction and dynamics of ionic liquids based on choline and amino acid anions, J. Chem. Phys. 142 (23) (2015).
[32] A. Le Donne, H. Adenusi, F. Porcelli, E. Bodo, Structural features of cholinium based protic ionic liquids through molecular dynamics, J. Phys. Chem. B 123 (26) (2019) 5568–5576.

[33] M. Campetella, A. Le Donne, M. Daniele, L. Gontrani, S. Lupi, E. Bodo, F. Leonelli, Hydrogen bonding features in cholinium-based protic ionic liquids from molecular dynamics simulations, J. Phys. Chem. B 122 (9) (2018) 2635–2645.
[34] A. Le Donne, H. Adenusi, F. Porcelli, E. Bodo, Hydrogen bonding as a clustering agent in protic ionic liquids: like-charge vs opposite-charge dimer formation, ACS Omega 3 (9) (2018) 10589–10600.
[35] M.V. Fedotova, S.E. Kruchinin, G.N. Chuev, Features of local ordering of biocompatible ionic liquids: the case of choline-based amino acid ionic liquids, J. Mol. Liq. 296 (2019).
[36] M. Moosavi, N. Banazadeh, M. Torkzadeh, Structure and dynamics in amino acid choline-based ionic liquids: a combined QTAIM, NCI, DFT, and molecular dynamics study, J. Phys. Chem. B 123 (18) (2019) 4070–4084.
[37] M. Deetlefs, C. Hardacre, M. Nieuwenhuyzen, O. Sheppard, A.K. Soper, Structure of ionic liquid-benzene mixtures, J. Phys. Chem. B 109 (4) (2005) 1593–1598.
[38] A.A. Rodriguez-Sanz, E.M. Cabaleiro-Lago, J. Rodriguez-Otero, On the interaction between the imidazolium cation and aromatic amino acids. A computational study, Org. Biomol. Chem. 13 (29) (2015) 7961–7972.
[39] S. Fujiwara, T. Ichikawa, H. Ohno, Cation-pi interactions within aromatic amino acid ionic liquids: a new tool for designing functional ionic liquids, J. Mol. Liq. 222 (2016) 214–217.